

Mask Characterization for Double Patterning Lithography

Karsten Bubke¹, Eric Cotte¹, Jan Hendrik Peters¹,
Robert de Kruif²,
Mircea Dusa³,
Joerg Fochler⁴, Brid Connolly⁴

¹ Advanced Mask Technology Center GmbH & Co. KG, Raehnitzer Allee 9, 01109 Dresden, Germany

² ASML Netherlands B.V., De Run 6501, 5504 DR Veldhoven, The Netherlands

³ ASML US Inc., Santa Clara, CA, USA 95054

⁴ Toppan Photomasks Inc., Raehnitzer Allee 9, 01109 Dresden, Germany

ABSTRACT

Double patterning (DPT) lithography is seen industry-wide as an intermediate solution for the 32nm node if high index immersion as well as extreme ultraviolet lithography are not ready for a timely release for production. Apart from the obvious drawbacks of additional exposure, processing steps and the resulting reduced throughput, DPT possesses a number of additional technical challenges. This relates to, e.g., exposure tool capability, the actual applied process in the wafer fab but also to mask performance and metrology. In this paper we will address the mask performance.

To characterize the mask performance in an actual DPT process, conventional parameters need to be re-evaluated. Furthermore new parameters might be more suitable to describe mask capability. This refers to, e.g., reticle to reticle overlay but also to CD differences between masks of a DPT reticle set. A DPT target of reticle to reticle induced overlay of 6nm, 3σ at mask level was proposed recently¹ for the 32nm node. The results show that this target can be met.

Besides that, local CD variations and local displacement become critical. Finally, the actual mask metrology for determination of these parameters might not be trivial and needs to be set up and characterized properly. In this paper we report on the performance of two-reticle sets based on a design developed to study the impact of mask global and local placement errors on a DPT dual line process.

In a first step we focus on reticle to reticle overlay. The overlay between two masks evaluated for different wafer overlay targets is compared with measurements on actual resolution structures. In a second step, mask to mask CD variations are addressed. Off-target CD differences as well as variations of CD signatures on both reticles of a set are investigated. Finally, local CD variations and local displacements are examined. To this aim, local variations of adjacent structures on the reticle are characterized. The contribution of local effects to the overall CD and registration budget is estimated.

Keywords: Double Patterning, Overlay, Registration, Mask Metrology

1. INTRODUCTION

There are currently three main options for the extension of lithography to half pitches smaller than ~40nm: high index immersion lithography, extreme ultraviolet (EUV) lithography and double patterning (DPT), each option having their specific advantages and drawbacks. Main problem of a further increase of the NA are material issues, namely the development of high index liquids and lens materials. The infrastructure for EUV lithography is currently still incomplete, making the insertion point of EUV uncertain. Besides considerable technical challenges, DPT seems economically not attractive because of the cost impact of doubling critical patterning steps. However, considering the aggressive shrink rates in particular of NAND flash products, DPT by some means or other will be required at least as an intermediate lithography solution.

The basic principle of DPT is the printing of a pattern with dimensions near or below the resolution limit by splitting the pattern into two or more complementary parts which are successively formed on wafer¹⁻⁷. For a simple lines and spaces

pattern this means that in a first step a pitch twice as large as the desired final pitch is formed, whereas the remaining structures are obtained after a second lithography and/or processing step.

At present, a number of different DPT options are areas of active research and development. The techniques currently under investigation may be subdivided into two groups:

- Photo Etch Photo Etch (PEPE) approaches¹⁻⁶: the layout is split into two less dense mask patterns, both patterns are successively exposed, developed and etched into auxiliary hard masks and finally transferred to the substrate. Two basic flows exist, the so called positive process printing lines and the negative process printing trenches. For each exposure a dedicated photomask is used.
- Spacer technology⁷: in a first step, lines with double pitch are processed in a hard mask, the pitch doubling is then obtained by conformal spacer deposition.

The two basic techniques described above possess a variety of different versions, each having their respective challenges and problems associated with it. For all PEPE techniques the final desired structure is made out of two patterns with each having its own mask and respective lithographic process. Therefore overlay between both patterns is essential. Overlay errors result in line or space CD errors depending on whether a positive or negative process is applied. A DPT target of reticle to reticle induced overlay of 6nm, 3σ at mask level was proposed recently¹ for the 32nm node. Furthermore, as the CD on wafer consists out of two populations, differences in mean CD between both patterns result in a larger overall CDU.

There are a number of different contributors to the overall error budget related to exposure tool capability, the actual applied process in the wafer fab but also to mask performance and metrology. In this paper, we will report on the characterization of DPT relevant mask parameters. The study is based on a reticle set with a design developed to study the influence of mask global and local placement errors on a DPT dual line process^{1,5}. Main emphasis is laid upon the characterization of mask to mask parameters. Furthermore, local displacements and CD variations as well as their contribution to the overall budget are addressed.

2. RETICLE SET – MASK DESIGN

A sketch of the design of the reticle set is shown in Fig. 1. Each mask consists of identical modules arranged in a 13x19 array over an area of around 10cmx13cm. The modules on each mask contain a variety of DPT structures, i.e. complementary parts of splitted features of the original layout. Furthermore, a number of different metrology targets are included at different locations. The reticle set was provided by TOPPAN Photomasks from the Mask Technology Center in Dresden. For the writing of the reticles an e-beam NuFlare 5000 was used.

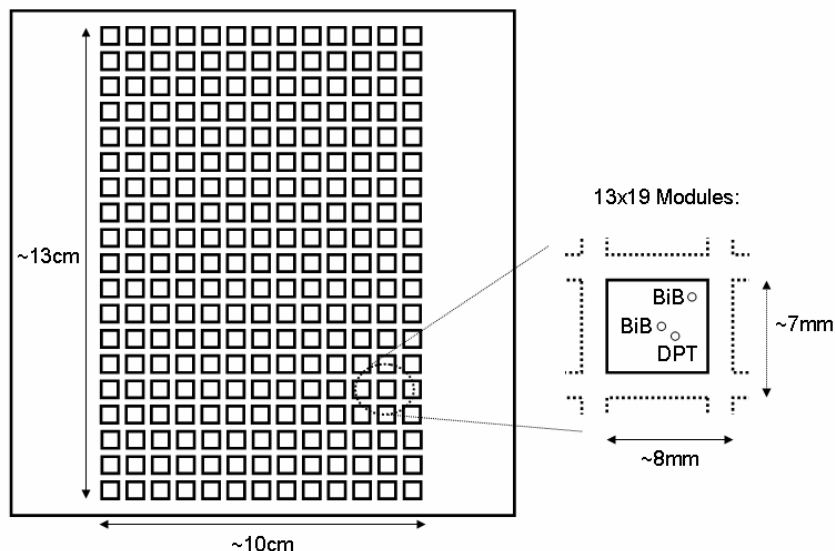


Figure 1: Sketch of the design of reticle set, relevant features in each module are explained in Fig. 2.

Of particular interest for this study are three features which are part of each module (see Fig. 2):

- Bar in Bar (BiB) overlay targets located near the center of each module;
- BiB targets near the corner of each module, the distance to the center target is 1.6mm in x-direction and 1.2mm in y-direction;
- Splitted gratings designed to be printed on wafer with a DPT dual line process. A sketch of these features is shown in Fig. 2. Gratings are located in close proximity (around 100 μ m in x and y) to the BiB marks near the center of each module. Identical vertically and horizontally (meaning 90° rotated) oriented structures are placed next to each other. The pitch of the structure under investigation is 640nm on mask corresponding to a final half pitch of 40nm (after DPT) on wafer. Each feature contains 10 lines with a specifically designed surrounding allowing CD and registration measurements of particular lines at particular locations on both mask and wafer. From hereon these features will be referred to as DPT structures.

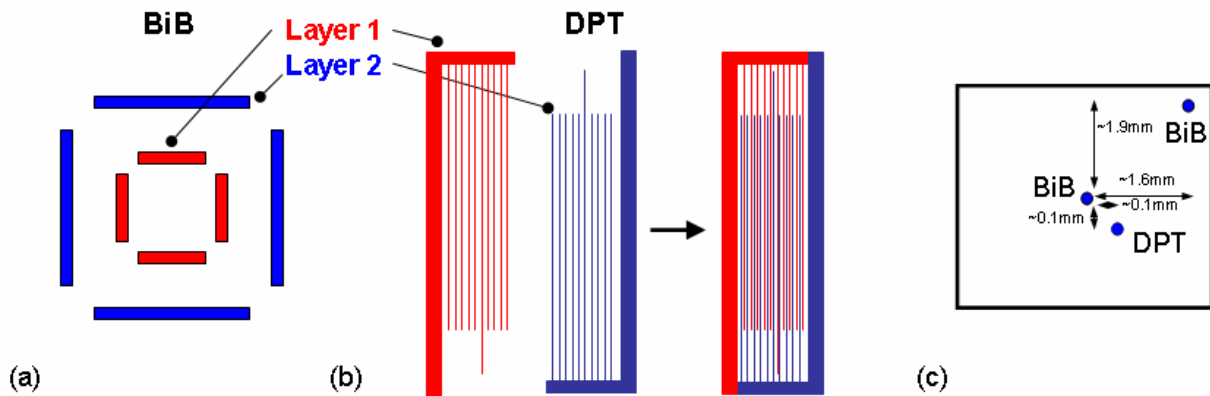


Figure 2: Features under consideration: (a) Bar in Bar (BiB) targets, (b) splitted gratings designed to be printed on wafer with a DPT dual line process – abbreviated “DPT structures”, (c) location of the features in each of the 13x19 modules (see also Fig.1).

3. CHARACTERIZATION OF RETICLE OVERLAY

It was recently shown that a proper characterization of reticle registration should be based on the measurement of targets at locations in the die area⁸. However, for a meaningful characterization of mask overlay it is also important to investigate the correlation between registration measured on standard targets with the displacement of the actual structures of interest. For DPT, as overlay errors translate directly into CD errors, these are e.g. the splitted features on each mask which end up as adjacent lines on wafer (as shown in Fig. 2(b)). Another important parameter is the maximum distance between resolution structures and overlay targets to obtain a reasonable correlation between both measurements.

All registration measurements on reticle were performed using a VISTEC IPRO3. The measurement principle is based on the imaging of mask structures onto a CCD-camera and a subsequent edge detection from the intensity profile. The resolution of the optics and hence the size of measurable structures is therefore limited. However, for the DPT structures considered here the resolution was sufficient although measurement recipes had to be adjusted to account for lower contrast. The reported x-displacements were measured on the center line of vertically and y-displacements on the center line of horizontally oriented features, respectively.

All reported data are corrected for translation, rotation and magnification in x and y independently as well as for non-orthogonality. For the characterization of overlay between both reticles we use the correlation coefficient R and the 3σ of the difference of registration of both masks as defined in the Appendix. The correlation coefficient, lying between -1 (anti correlated) and 1 (perfectly correlated), is a suitable means for the description of matching of both registration maps.

Correlation of Registration Targets on same Mask

In a first step we compare the results of registration measured on BiB targets with the registration measured on the DPT structures. Respective data are shown in Fig. 3. L1 and L2 refer to Layer 1 (reticle 1) and Layer2 (reticle 2), respectively. The measured registration results are in the order of 5-6nm 3σ taken over 13 x 19 measured positions for each feature. These values contain also the measurement error. For both reticles the obtained displacements measured on DPT structures are similar to the values obtained from BiB overlay targets.

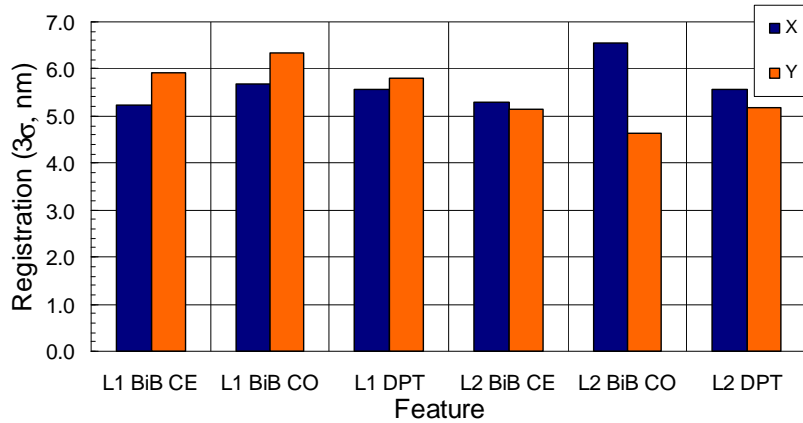


Figure 3: Registration (3σ , nm) measured on both reticles (Layer1 – L1, Layer2 - L2) on different structures at different locations: BiB CE- Bar in Bar near the center of module, BiB CO – Bar in Bar at the corner of module, DPT – splitted grating near the center of module.

Having found that the values of 3σ registration are comparable for BiB targets and DPT structures, in a next step we compare the correlation of respective registration maps. Correlation coefficients, similarly defined as in the Appendix, are given in Fig. 4.

The correlation between the y-displacements of both masks show the expected behavior. Structures in close proximity, i.e. BiB center and DPT structures, correlate fairly well whereas the correlation decreases as the distance between structures increases. The correlation between the x-displacements is generally poor. This also applies to the correlation between DPT structures and BiB center targets that are placed closely together at a distance of $\sim 100\mu\text{m}$.

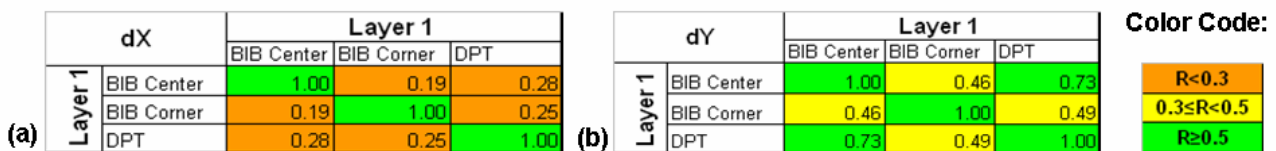


Figure 4: Correlation coefficients of registration data measured on features shown in Fig. 2 (Layer1): (a) x-displacements, (b) y-displacements.

It is useful to look more closely at the different contributions to mask registration errors. Measured registration and CD data always consist of a deterministic or systematic part and noise. The deterministic part may have contributions on different spatial scales: a global signature for which the sampling scheme chosen here is appropriate, intermediate spatial scales and finally local displacements, e.g. line to line registration errors. The part which can be described by a global signature should lead to a good correlation between different targets in close proximity.

A technique which can be used to separate the spatial fingerprint from statistical noise is thin plate spline smoothing (TPS). The method has been successfully applied to both CD data¹⁰ and registration data¹¹ in the past. Fig. 5 shows the registration map of one mask based on the BiB targets in the center of each module and on the DPT structures as well as

their respective signatures obtained from TPS smoothing. There clearly exists a global fingerprint which is comparable for both the BiB targets and DPT structures - the correlation coefficients between both signatures are large for both x- and y-displacements. One should note that only the smooth systematic part of registration data is obtained, the remainder being fast varying signatures and noise. The 3σ value of the remainder is around 4nm for x- and y-displacements, which is a significant portion of the registration errors (which are around 5-6nm 3σ).

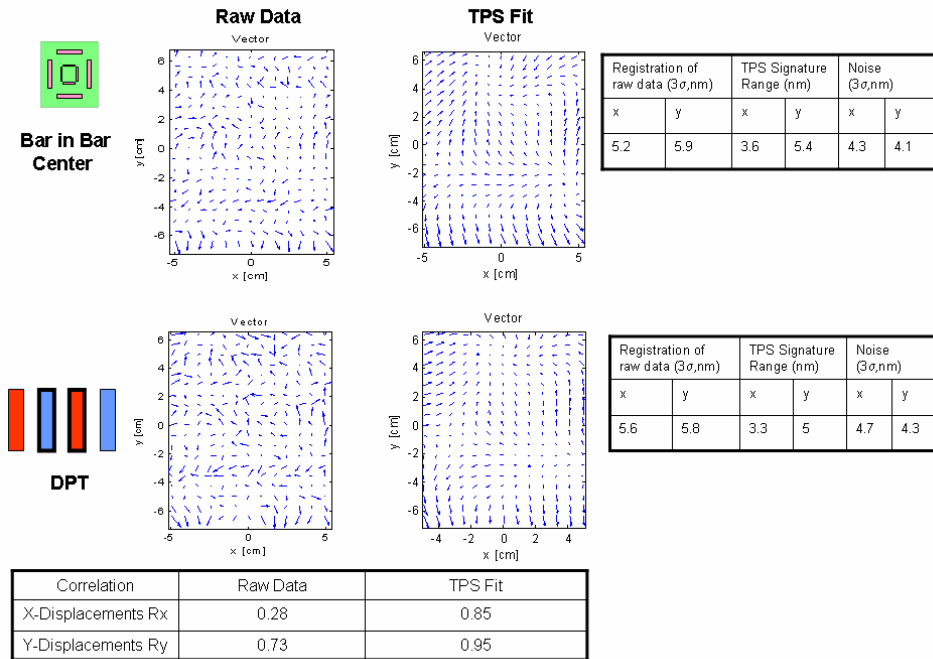


Figure 5: Vector plots of raw and smoothed data (smoothing via TPS) measured on Bar in Bar targets and DPT structures located in close proximity, as well the corresponding correlation between raw and smoothed data; also given are the registration value of raw data, the range of TPS fit and the 3σ of the remainder. The table at the bottom of the figure gives the accompanying correlation coefficients.

Finally we address contributions to the overall registration on the smallest spatial scale, meaning the placement error of two adjacent lines. For this, the displacements of 3 adjacent lines in the middle of the DPT structures were measured with the IPRO. Corresponding data can be found in Fig. 6.

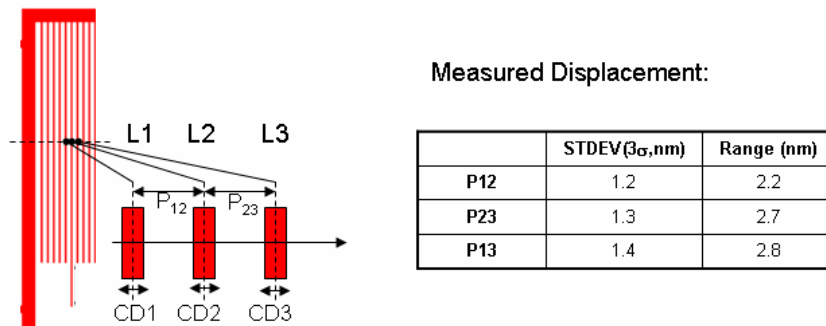


Figure 6: Measured displacement between individual lines in the center of the DPT structure.

Local displacements reported in Fig. 6 are deviations from the nominal pitch of 640nm. The measured deviations are in the order of $\sim 1.3\text{nm } 3\sigma$. Considering the fact that these values contain also measurement noise, the local displacement of particular lines is well within $1\text{nm } 3\sigma$ and hence does not contribute to a large extend to the overall registration error.

Reticle to Reticle Overlay

In the previous subsection we looked at the registration error on the individual masks measured on different features. In this subsection we will focus on mask to mask overlay. Fig. 7 shows the correlation of registration of both masks for different features. The correlation between both masks measured on the same features is generally good. Correlation coefficients of ~ 0.7 and ~ 0.5 are obtained for x- and y-displacements, respectively. One reason for this large correlation is certainly the similarity of the layouts and hence loadings of both masks. Similar to the registration data shown in Fig. 4, the correlation is poor for X data obtained from different features. This can again be explained by a large contribution of very local signature variations to the overall registration. Variations are less pronounced for y-displacements.

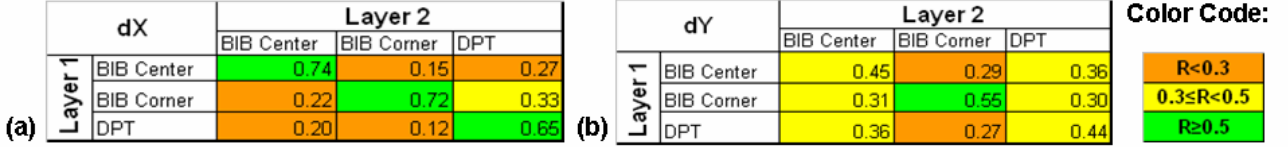


Figure 7: Correlation of registration measured on both masks, for different features: (a) x-displacements, (b) y-displacements.

Fig. 8 shows the actual 3σ values of mask to mask overlay measured on the features from the same type on both masks. The obtained results are similar for DPT structures and BiB targets and amount to 4-5nm 3σ in x- and 5-6nm 3σ in y-direction, respectively.

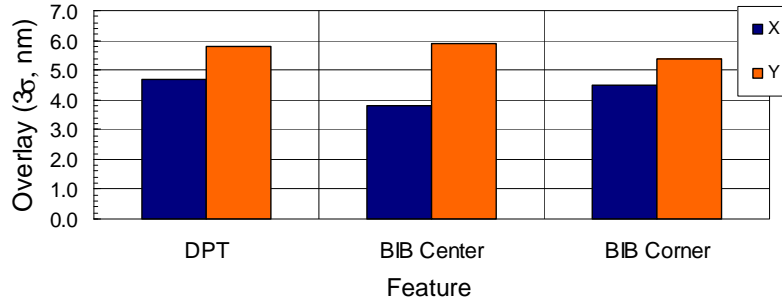


Figure 8: Mask to mask overlay measured on various features: comparison of DPT structures with BiB targets.

Whereas global signatures on masks offer the possibility of the application of certain correction schemes¹¹, variations on small spatial scales are more difficult or even impossible to correct for. It is therefore interesting to look at the contribution of systematic parts of registration on both masks to the overall overlay budget. As described in the previous subsection, the registration on each mask can be divided into a systematic part on large spatial scales dx_{sys} and a residual part dx_{res} . The overlay is then given by (written for x-displacements only),

$$OVL_x = dx1_{sys} + dx1_{res} - (dx2_{sys} + dx2_{res}), \quad (1)$$

where $dx1$ and $dx2$ are the displacements on Layer 1 and Layer 2, respectively. The accompanying standard deviation can be written as,

$$\sigma_{OVL_x} = \sqrt{\sigma_{sys}^2 + \sigma_{res}^2} = \sqrt{\sigma_{dx1sys}^2 + \sigma_{dx2sys}^2 - 2R_{sys1/2}\sigma_{dx1sys}\sigma_{dx2sys} + \sigma_{res}^2}, \quad (2)$$

where σ_{sys} and σ_{res} are the standard deviations of the systematic and the residual part, respectively. $R_{sys1/2}$ denotes the correlation between the systematic parts of layer 1 and layer 2, respectively. The residual part σ_{res} may contain both fast varying signatures and statistical noise. Cross correlations between the systematic and residual part of registration dx_{sys} and dx_{res} are small (data not shown here).

[nm]	$3\sigma_{OVL}$	$3\sigma_{d1sys}$	$3\sigma_{d2sys}$	$R_{sys1/2}$	$3\sigma_{sys}$	$3\sigma_{res}$
X	4.7	2.1	2.4	0.84	1.3	4.5
y	5.8	3.1	2.2	0.91	1.5	5.6

Table1: Different contributions to mask to mask overlay measured on DPT structures: σ_{OVL} – standard deviation of overlay; $\sigma_{d1/2sys}$ – standard deviations of signatures of layer 1 and layer 2, respectively; $R_{sys1/2}$ – correlation coefficient of signatures on both layers; σ_{sys} – resulting standard deviation of the systematic contributions to overlay; σ_{res} – standard deviation of remainder.

In Table 1 respective values are given for DPT structures. The correlation between large scale systematics of both masks, $R_{sys1/2}$, is considerably larger than the values obtained for the overall registration stated in Fig. 7. Again, this good match between global signatures can be partially attributed to the similar layout of both masks. Maps of registration of both masks before and after application of thin plate spline smoothing are shown in Fig. 9. The overall contribution of signatures from both masks to overlay is small due to large correlation. The data imply that for a significant improvement of overlay beyond the values given here registration on intermediate scales need to be investigated and reduced. This, in particular, refers to future mask writing tools.

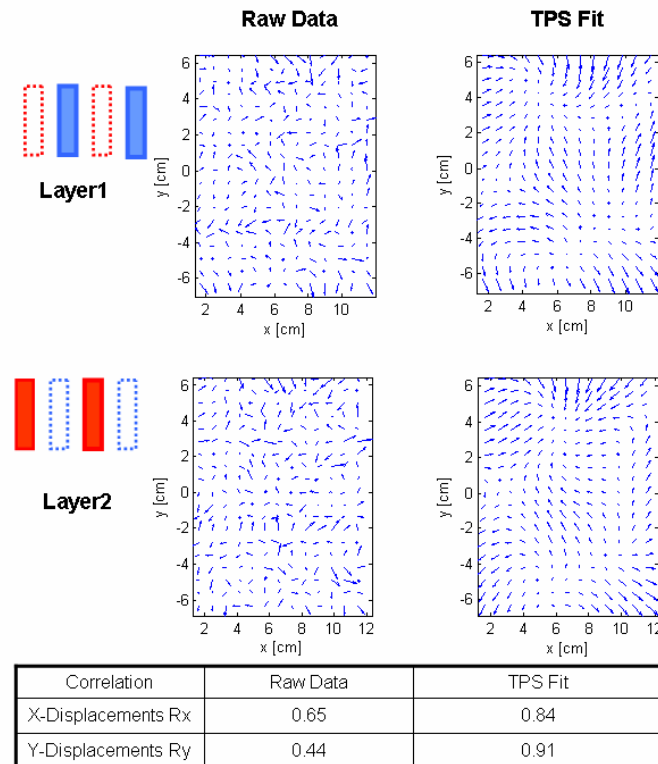


Figure 9: Registration maps of DPT structures on reticle 1 (Layer 1) and reticle 2 (Layer 2) before and after application of thin plate spline (TPS) smoothing. The table at the bottom of the figure gives the accompanying correlation coefficients.

4. CHARACTERIZATION OF CD PERFORMANCE

Besides overlay there are additional challenges associated with DPT that are related to CD. Specific to DPT processes considered here is the presence of two CD populations on wafer¹. Apart from scanner and process contributions, the

mask can also contribute a certain amount to the overall CD error budget. As a result, the mean-to-target difference for two masks used as a double patterning set was added to the ITRS roadmap just recently¹². Apart from small differences in CD mean values, for certain applications it can be advantageous to have similar CD signatures on both masks.

Fig. 10 shows respective data of the DPT reticle set considered here. CD's were measured at the centerline of the DPT structures (see Fig. 6). Very good off-target performance is obtained with a mean-to-target difference well within the measurement noise. For the CD signatures the TPS fit of respective data are shown. The signatures of both reticles are very similar with a correlation coefficient R of ~0.9. The maximum deviation of the smoothed CD maps is around 2nm.

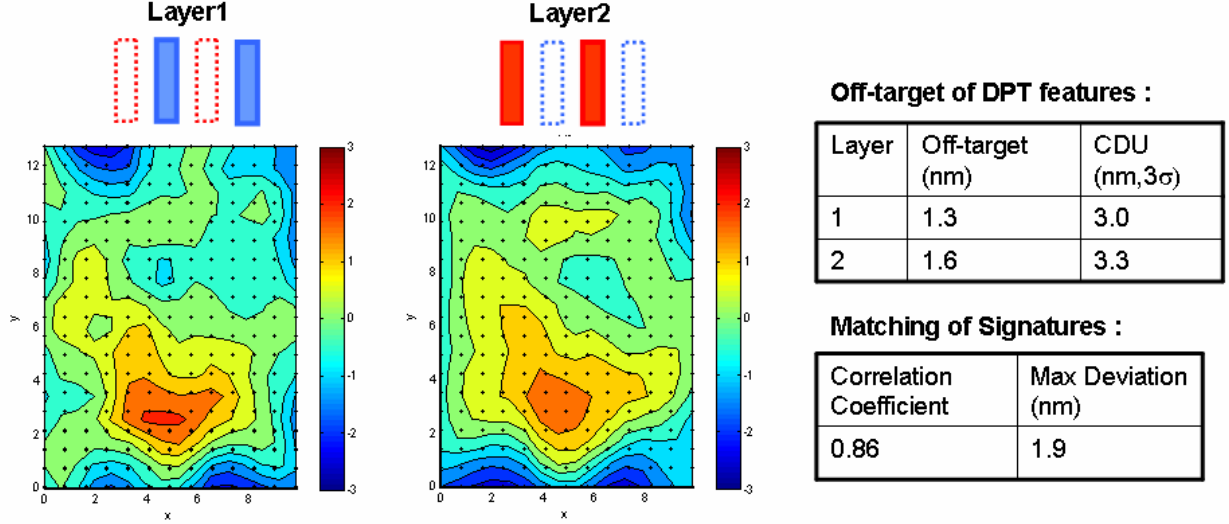


Figure 10: CD signatures of DPT structures on both layers, CD maps are shown after application of thin plate spline smoothing; also included are off-target values; for the characterization of signature differences the correlation coefficient as well as the maximum deviation between CD maps is given (all data mask scale).

To investigate the contribution of local CD variations to the overall CD uniformity we performed CD measurements on particular lines of the DPT structures. The actual locations are identical to the ones investigated for local displacements sketched in Fig. 6. Respective data are given in Table 2. The 3σ of measured CD differences is ~2.3nm. However, one should keep in mind that this value contains measurement noise and contributions from line edge roughness (LER). The separation of real displacements from metrology and LER is not trivial.

To investigate the different contributions to the overall CD data, we use TPS to separate the deterministic part from noise. The global signature CD_{sys} obtained from two adjacent lines should be equal, which can be written as,

$$CD_1 = CD_{\text{sys}} + CD_{\text{noise1}}, \text{ and } CD_2 = CD_{\text{sys}} + CD_{\text{noise2}}. \quad (2)$$

The 3σ of the differences between two lines can therefore be expressed in terms of TPS noise as,

$$3\sigma_{CD1-CD2} = 3\sqrt{\sigma_{\text{noise1}}^2 + \sigma_{\text{noise2}}^2}. \quad (3)$$

If the noise of the TPS fit contains large contributions of fast varying CD signatures, i.e. CD on intermediate scales, then the calculated value of Eq. (3) should be larger than the 3σ value of measured local CD differences. In Table 2 respective data can be found. There is a good match between measured CD differences and values obtained from TPS. This implies that, unlike what has been found for the registration data, CD variations on intermediate scales are rather small.

	Measured STDEV (3 σ ,nm)	Range (nm)	STDEV obtained from TPS (3 σ ,nm)
CD1-CD2	2.3	4.6	2.0
CD2-CD3	2.4	4.3	1.9
CD1-CD3	2.3	4.1	2.2

Table 2: Standard deviation and range of measured CD differences of adjacent lines; also included standard deviation of CD differences obtained from TPS fit according to eq. (3).

5. SUMMARY AND CONCLUSIONS

We investigated the overlay and CD performance of a reticle set intended for a double patterning dual line process.

Registration measurements on a standard overlay target, a Bar-in-Bar feature, and at resolution DPT features yield comparable values of 5-6 nm 3 σ . This implies that the used standard target represents the registration quality of other features and can be used as an overall indicator of the quality of registration of the reticle. However, the correlation of registration data obtained on different features was found to be poor even for structures in close proximity. Data analysis using thin plate spline modeling shows that a large part of the overall registration can be attributed to variations on intermediate spatial scales. Local displacements were found to be well below 1 nm 3 σ and have as such very limited contribution to the overall registration error.

Reticle to reticle overlay measured on the same structures on both masks was found to be around 5 nm 3 σ . The recently proposed target¹ of a reticle to reticle induced overlay of 6nm, 3 σ (or 1.5nm at wafer level) for the 32nm node was met for the reticle set investigated in this paper.

The distance between the locations of targets has an impact on the obtained overlay. Therefore a reticle to reticle overlay measurement should be performed on the same locations on both plates. For the reticles considered here the contribution of global signatures to the overall overlay value was found to be small. The remainder of 4-5nm 3 σ is partially due to registration on intermediate scales. This, e.g., refers to the mask writing tool.

The CD signatures obtained on both plates showed a good correlation and a very small mean to target difference. Local CD variations measured on particular lines were found to be in agreement with the noise level of a thin plate spline modeling of data. This indicates that, unlike to what was obtained for registration data, CD variations on intermediate spatial scales are rather small.

APPENDIX

Registration is defined as the difference (dx,dy) between the actual position of a feature and its nominal design position. Overlay is a measure for the discrepancy between two registration maps and is simply defined as the difference (dx1-dx2,dy1-dy2) between registration at particular positions. Specifications on registration are usually given in terms of the standard deviation defined as,

$$\sigma_{dx} = \sqrt{\frac{1}{N-1} \sum_i (dx_i - \overline{dx})^2}, \quad (1)$$

where dx_i denotes the registration error at a particular position and \overline{dx} the average of all measured values. The standard deviation of overlay between two reticle sets can be expressed in terms of the registration as,

$$\sigma_{OVLx} = \sqrt{\sigma_{dx1}^2 + \sigma_{dx2}^2 - 2R_x \sigma_{dx1} \sigma_{dx2}}, \quad (2)$$

where the correlation coefficient R_x is defined as ,

$$R_x = \frac{\sigma_{dx1dx2}}{\sigma_{dx1}\sigma_{dx2}}, \text{ with the covariance given by } \sigma_{dx1dx2} = \frac{1}{N-1} \sum_i (dx1 - \overline{dx1})(dx2 - \overline{dx2}). \quad (3)$$

Whereas (1)-(3) are written for x-displacements, there are obviously analogous expressions for y-displacements. Assuming the registration performance of both plates to be at least similar $\sigma_{dx1} \approx \sigma_{dx2}$, the overlay amounts to,

$$\sigma_{OVLx} = \sigma_{dx} \sqrt{2(1-R_x)}. \quad (4)$$

Hence, for good overlay between reticles both small registration and good correlation are beneficial. The correlation coefficient lies between 1 and -1. Values close to 1 correspond to good matching between plates resulting in a small overlay. Values close to -1 correspond to anti correlated displacements with maximum overlay of $\sigma_{OVLx} \approx 2\sigma_{dx}$.

ACKNOWLEDGEMENTS

AMTC is a joint venture of Infineon, AMD and Toppan Photomasks and gratefully acknowledges the financial support by the German Federal Ministry of Education and Research (BMBF) under Contract No. 01M3154A ("Abbildungsmethodiken für nanoelektronische Bauelemente"). In Dresden, we thank Andreas Nimz, Michael Geller, Jens Rudolf, Gunter Antesberger and Jan Richter for support. At ASML we thank Judith van Praagh, Onno Wismans and Marcel Demarteau for the reticle design and design support.

REFERENCES

1. M. Dusa et al., „Pitch doubling through dual-patterning lithography challenges in integration and litho budgets“, *Proceedings of the SPIE*, vol. 6520, 2007.
2. G. Capetti et al., “Sub-k1 = 0.25 lithography with double patterning technique for 45-nm technology node flash memory devices at $\lambda = 193\text{nm}$ ”, *Proceedings of the SPIE*, vol. 6520, 2007.
3. Seo-Min Kim, Sun-Young Koo, Jae-Seung Choi, et al., “Issues and challenges of double patterning lithography in DRAM“, *Proceedings of the SPIE*, vol. 6520, 2007.
4. Chang-Moon Lim, Seo-Min Kim, Young-Sun Hwang, et al., ”Positive and negative tone double patterning lithography for 50nm flash memory”, *Proceedings of the SPIE*, vol. 6154, 2006.
5. M. Maenhoudt, J. Versluijs, H. Struyf, J. Van Olmen, M. Van Hove, “Double patterning scheme for sub-0.25 k1 single damascene structures at $\text{NA}=0.75$, $\lambda=193\text{nm}$ ”, *Proceedings of the SPIE*, vol. 5754, 2004.
6. C. Noelscher et al., “Double line shrink lithography at $k1=0.16$ ”, *Microelectronic Engineering* 4864, February 2006.
7. Woo-Yung Jung, Sang-Min Kim, Choi-Dong Kim, et al., ”Patterning with amorphous carbon spacer for expanding the resolution limit of current lithography tool“, *Proceedings of the SPIE*, vol. 6520, 2007.
8. Bernd Schulz, Rolf Seltmann, Jens Busch, et al., “Meeting overlay requirements for future technology nodes with in-die overlay metrology“, *Proceedings of the SPIE*, vol. 6520, 2007.
9. Eric Cotte, Benjamin Alles, Timo Wandel, et al., “193-nm immersion photomask image placement in exposure tools”, *Proceedings of the SPIE*, vol. 5992, 2005.
10. Clemens Utzny, Martin Rößiger, “Determination of spatial CD signatures on photomasks”, *Proceedings of the SPIE*, vol. 6349, 2006.
11. B. Alles, B. Simeon, “Data evaluation as source for modeling in nano-imaging”, ARGESIM Report no. 30, MATHMOD 2006.
12. International Technology Roadmap for Semiconductors, 2007 edition, <http://public.itrs.net>.